HHS Public Access

Author manuscript

J Cell Biochem. Author manuscript; available in PMC 2018 November 01.

Published in final edited form as:

J Cell Biochem. 2017 November ; 118(11): 3920–3931. doi:10.1002/jcb.26045.

PHOSPHOLIPIDOMIC STUDIES IN HUMAN CORNEA FROM CLIMATIC DROPLET KERATOPATHY

M. Fernanda Suarez[1], **M. Carmen Piqueras**[2], **Leandro Correa**[3], **Evangelina Esposito**[3], **M. Fernanda Barros**[3], **Sanjoy K. Bhattacharya**[2], **Julio A. Urrets-Zavalia**[3,#], and **Horacio M. Serra**[1,*,#]

[1]CIBICI-CONICET, Department of Clinical Biochemistry, Faculty of Chemical Sciences, Universidad Nacional de Cordoba, Argentina

[2]Bascom Palmer Eye Institute, University of Miami Miller School of Medicine, Miami, Florida

[3]Department of Ophthalmology, University Clinic Reina Fabiola, Universidad Catolica de Cordoba, Argentina

Abstract

Climatic droplet keratopathy (CDK) is an acquired degenerative disease predominantly affecting males over 40 years old. It results in progressive corneal opacities usually affecting both eyes. CDK is multifactorial and its etiology remains unknown. Our recent findings are consistent with CDK pathology being driven by environmental factors with oxidative stress playing an important role (for example, contributing to lipid peroxidation) rather than climate factors. The changes in corneal lipid composition affected by environmental factors remain understudied. The purpose of this study was to systematically investigate phospholipids profile [phosphatidylcholine (PC) and phosphatidylserine (PS)] in corneas from CDK patients using tandem mass spectrometry. Samples from CDK areas and from non-affected areas were obtained from patients diagnosed with CDK who underwent cataract surgery, were subjected to lipid extraction using a modified Bligh and Dyer method; protein concentrations were determined using the Bradford's method. Lipids were identified and subjected to ratiometric quantification using TSQ Quantum Access Max triple quadrupole mass spectrometer, using appropriate class specific lipid standards. All phospholipid classes showed lower total amounts in affected areas compared to control areas from CDK's corneas. Comparative profiles of two phospholipid classes (PC, PS) between CDK areas and control areas showed several common species between them. We also found a few unique lipids that were absent in CDK areas compared to controls and vice versa. Lower amount of phospholipids in CDK areas compared to control areas could be attributed to the lipid peroxidation in the affected corneal regions as a consequence of increased oxidative stress.

[*]Corresponding author: Horacio Marcelo Serra., CIBICI-CONICET, Department of Clinical Biochemistry, Faculty of Chemical Sciences, Universidad Nacional de Cordoba, Haya de la Torre esquina Medina Allende, 5000, Cordoba, Argentina., Phone: 54 (351) 535-3851, Fax: 54 351 4333048. hserra@fcq.unc.edu.ar.

[#]: The last two authors equally contributed to this work.

CONFLICT OF INTERESTS

The authors declare that there is no conflict of interests regarding the publication of this paper.

Keywords

CDK; Phospholipids; Phosphatidylcholine; Phosphatidylserine; Cornea; Tandem mass spectrometry

Climatic droplet keratopathy (CDK) is a bilateral degenerative corneal disease related to advanced age, lifestyle, and multiple environmental factors such as corneal micro traumas, low humidity and lack of adequate protection for exposure to ultraviolet radiation (UVR) (Suarez et al., 2015). CDK most commonly affects males over 40 years old, in the form of progressive opacities of the anterior layers of the cornea. This disease is rare in temperate latitudes, and it is commonly linked to overexposure to UVR, being endemic in certain rural communities around the world. Since the first description of the disease in 1898 (Baquis), CDK has been reported in different parts of the world following different criterions (presumed aetiology, geographic area, by eponym, clinical presentation, nature of corneal deposits and patient's activities) and more recently in the Patagonia region of Argentina, as has been reviewed by Serra et al. (2015).

CDK slowly progresses to corneal opacity, through three grades of increasing severity. In the initial stages (grade 1), multiple tiny and tightly confluent translucent extracellular sub epithelial deposits, located in the Bowman layer close to the temporal and/or nasal limbus, giving the affected cornea a tarnished, hazy aspect. In grade 2, haziness spreads over the inferior 2/3rds of the cornea, affecting the central cornea. At this stage, visual acuity may be moderate to severely affected due to the visual axis involvement. Grade 3 is characterized by the presence of large golden sub-epithelial droplets of different sizes (some of them are 1 mm in diameter) grouped in clusters that grow and cover the cornea as the disease progresses. In advanced cases, areas of vascularized anterior stromal opacification or fibrosis may be observed. In general, corneal sensitivity and visual acuity are severely affected at this stage (Freedman, 1965; Urrets-Zavalia et al., 2007).

Another clinical finding observed in some of our patients in the Argentinian Patagonia is a mild to severe atrophy of the 1/2 inferior iris stroma, more frequently observed in grades 2 and 3 (Urrets-Zavalía et al., 2007). Despite the harsh environmental conditions in which individuals from this region live, dry eye was not common among CDK patients, or controls (Urrets-Zavalía et al., 2007).

We have investigated the biological features of matrix metalloproteinases (MMPs) and their inhibitors TIMPs in patients with CDK, as these molecules control the degradation of the corneal epithelium and stroma. Our studies showed enhanced MMP-2 and MMP-9 levels and a decreased expression of TIMP-1 in CDK patients' tears (Holopainen et al., 2011). Immunohistochemistry showed that MMP-2 was expressed at the basement membrane zone in both control and affected corneas, but also marked the edges of the granular CDK deposits; MMP-9 expression was restrained to basal layers of the epithelium and was markedly induced in CDK corneas (Holopainen et al., 2012). We also investigated the effect of UVR in the production of MMPs and cytokines using an *in vitro* cellular model of immortalized human corneal epithelial cells (HCE). Exposure of HCE cells to UVR

significantly increased MMP and pro-inflammatory cytokine secretion, suggesting an active participation of the corneal epithelium on CDK's pathogenesis (Holopainen et al., 2012).

Many advances that could help to understand ethiopathogenic mechanisms involved in CDK have been made in the last years, recently reviewed by Serra et al (2015).

Lipids constitute a unique group of biomolecules that mediate a large number of functional and structural activities in the cell, tending to maintain homeostasis (Checa et al., 2015), and constitute about 5% of the weight of mammalian cells (Fahy et al., 2009). Cellular lipids are highly complex and dynamic (Yang and Han, 2016). There is evidence that phospholipids may play an important role in the regulation of several ocular homeostatic mechanisms due to their presence in aqueous humor and subsequent changes under injury conditions (Liliom et al., 1998). Lipids are also important components of the tear film. The lipid layer is highly organized, consisting of a monolayer of phospholipids at the water-air interface, which provides a hydrophobic interface on which non-polar lipids expand (Rantamäki et al., 2011). Defects in the lipid layer of the tear film results in increased evaporation, which perpetuates ocular surface inflammation and damage. Also, lipids have been involved in ocular surface pathologies such as dry eye, allergic keratoconjunctivitis, infections and glaucoma (Ham et al., 2004; Robciuc et al., 2014; Fujishima et al., 2013; Aribindi et al., 2013a; Edwards et al., 2014).

There are no previous reports on identification or determination of superficial corneal lipid composition of patients with CDK. Lipid peroxidation may occur at the epithelium of the cornea exposed to prolonged exposure to UVR without adequate protection, in certain individuals under certain circumstances, which could result in an oxidative stress. Our aim was to systematically study lipids in corneal epithelial cells from CDK corneas using tandem mass spectrometry, and identify a differential composition, if any, between healthy corneal epithelial areas and CDK affected areas.

MATHERIAL AND METHODS

Tissue samples procurement

The samples were procured according to the protocol approved by institutional review process and the tenets of the Declaration of Helsinki. Corneal epithelial cell specimens from the eyes of two CDK patients (a 62-year old and 63-year old males) (Figure 1) at the moment of a planned cataract surgery were obtained and kept at −70° C until they were further processed. One CDK affected area, and one control non-affected area, were collected by scraping these regions of the cornea using a crescent knife. No abnormalities of the iris were observed biomicroscopically, and the ocular tensions, as well as the ocular fundus were normal in both eyes patients.

Lipid extraction

Corneal tissue was subjected to lipid extraction using a modified Bligh and Dyer method (Iverson et al., 2001). The organic phase with extracted lipids was dried in a Speed-Vac (Model 7810014, Labconco, Kansas City, MO, USA). Samples were flushed with argon gas to prevent oxidation. All extractions and subsequent handling were made using glass vials;

polyvinyl plastic was avoided completely to prevent contaminating impurities. Corresponding aqueous phase extracted proteins were subjected to determination of concentration using Bradford's method (Bradford, 1976), and these concentrations were used to normalize lipids per amount of proteins.

Mass spectrometry

Dried lipid samples were re-suspended in LC-MS grade Acetonitrile: Isopropanol (1:1). Samples were infused with a flow rate of 5μl/min, using Tri Versa Nanomate (Advion Inc., Ithaca, NY, USA), a chip-based electrospray ionization machine controlled with Chipsoft8.3.3 version software.

A triple quadrupole electrospray mass spectrometer (TSQ Quantum Access Max; Thermo Fisher Scientific, Pittsburgh, PA, USA) was used for analysis of lipids in infusion mode using TSQ Tune software that is part of the Xcaliber 2.3 software package. Samples were analyzed for 2.00 minutes with a 0.500-second scan. Scans typically ranged from 200 to 1000 m/z. A peak width was set at 0.7 and collision gas pressure was set at 1 mTorr. Sheath gas (nitrogen) was set to 20 arbitrary units. Auxiliary gas (Argon) was set to 5 arbitrary units. Settings for analyses of different phospholipid classes were established based on previous studies (Enriquez-Algeciras and Bhattacharya, 2013). The 0.1% formic acid (FA) was used as an additive method for analyses of lipids in the positive ion mode only (that is, for analyses of PC but not for PS). Control and CDK corneal epithelial cells were utilized for each of the two different class of phospholipid analyzed. Class specific lipids were quantified using class specific quantitative lipid standards:1,2-ditridecanoyl-*sn*-glycero-3-phosphocholine and 1,2-dioleoyl-*sn*-glycero-3-phospho-L-serine (sodium salt) (Avanti Polar Lipids, Inc; Alabaster, AL, USA). Approximately 5 scans each with and without internal standard (usually in the range of 0.1–10pmol) were performed for each sample. Ratiometric quantification was achieved using the MZmine 2.9 program. Lipid concentration was normalized to protein amount determined from the corresponding aqueous phase as described above.

Representative spectra for each sample were carefully and manually inspected by two independent observers from 5 spectra collected for each sample with and without the internal standard (total 10 spectra) and then used for further analyses. Spectra were converted to netCDF files from Thermo RAW files using the Xcalibur 2.3 software suite, subsequently imported into MZmine 2.9 (Edwards et al., 2014). Identification was carried out against a custom database created from the Lipid Maps Database (LMDB).

Identified lipids were subjected to analysis for determination of common and unique species using an Excel macro (Aribindi et al., 2013b). We defined unique when a given lipid species was found in only one group (control areas or CDK affected areas). Common species are those that have been found in samples from both control and CDK affected areas of both patients. All unique lipid experimental readings (the amount of lipid species pM/μg protein) were found to be significantly different from 0.0 by one sample t-test ($p \leq 0.05$).

Statistical analysis

Student's t-test was used for comparison between lipid concentrations in control areas vs CDK affected areas. A p-value ≤0.05 was considered significant.

RESULTS

We obtained lipid profiles for two classes of phospholipids: phosphatidylcholine (PC) and phosphatidylserine (PS), using established parameters (Enriquez-Algeciras and Bhattacharya, 2013). A representative PC and PS spectrum for control corneal samples without and with ratiometric standards (Fig. 2 A, 3A and Fig. 2 B, 3B, respectively) are shown. Using Excel Macros all data from two phospholipids were analyzed to determine the presence of common and unique lipid species in control areas and CDK affected areas.

All phospholipids classes showed higher total amounts in control areas compared to CDK affected areas. In grade 1, total phospholipids amount was 7.6 times higher in control than in CDK areas. In grade 2, phospholipids concentration was 35 times higher in control areas than in CDK affected areas. PC and PS concentrations were higher in the control than in CDK area in grade 1 (4.7 times and 10 times, respectively) as well as in grade 2 (5.7 times and 36 times, respectively). The total amount of all two classes of phospholipids normalized to total amount of proteins in the corresponding aqueous phase extractions are presented in table 1.

We found 35 unique PC species in the control areas and 38 species in CDK affected areas from grade 1 patient's sample. No unique PC species were found in samples from grade 2 (table 2, figure 4). For common lipids, we found 47 common PC species in control and CDK affected areas in grade 1 and 85 common PC species for grade 2 (table 3, figure 4).

In case of PS, 13 unique species were found in control areas and 8 in CDK affected areas from grade 1. For grade 2, 19 PS and 9 PS species were found in control and CDK areas, respectively (table 2, figure 4). Forty PS and 36 species were common between control and affected areas from grade 1 and grade 2, respectively (table 3, figure 4).

DISCUSION

CDK is a rare corneal degenerative disease characterized by progressive opacity because of accumulation of translucent material in the Bowman layer of the cornea within the interpalpebral fringe (Gray et al., 1992; Urrets-Zavalía et al., 2006, 2007). We have previously shown that CDK occurred in individuals who have lived their entire life under certain unfavorable environmental conditions such as high exposure to UVR, chronic micro erosions of the cornea, low levels of ascorbic acid (AA) in their diets and serum, and lack of protection with sunglasses or hats (Suarez et al., 2015). For those reasons we have previously proposed that this corneal disease should be call environmental proteinaceous corneal degenerative disease instead of climatic droplet keratopathy (Suarez et al, 2015).

The precise chemical nature of globules accumulated under the corneal epithelium remains uncertain despite many efforts have been made to unravel its composition (Tabbara, 1986; Kaji et al., 2007; Menegay et al., 2008; Kaji et al., 2010). It has been suggested that corneal

deposits are derived from plasma proteins that, after reaching an inflamed cornea from the limbal vessels, are degraded by excessive exposure to UVR (Gray et al., 1992). Although no mechanistic link between UVR exposure and CDK has been established, Holopainen et al. have addressed this issue analyzing tears and corneal specimens obtained from CDK affected eyes. They found that CDK samples have higher levels of MMP-2, MMP-9, and pro inflammatory cytokines than unaffected individuals (Holopainen et al., 2012). They hypothesized that these proteins are produced by the corneal epithelium, and showed that UVR-B is capable of inducing pro-inflammatory response in these cells with concomitant increase in MMP-2 and MMP-9 levels. This is then likely to increase the apoptotic/ necrotic response of the corneal epithelial cells, harm the integrity of the basement membrane, and, eventually, lead to visible changes in the corneal architecture.

Recently, we performed a study in which two groups of guinea pigs were exposed during 30 months to daily doses of UVR-B similar to the one received by CDK patients living in Patagonia Argentina, fed with AA sufficient or AA partially deficient diets, respectively. Superficial corneal debridement wounds were made in one eye using a rotating burr (Algerbrush II, Ambler Surgical, Exton, PA, USA) at the nasal or temporal corneal limbus (once a week, alternating each region) previous topical anesthetic applied on the ocular surface (proparacaine ophthalmic solution, Alcon laboratories Argentina, Buenos Aires, Argentina). We found that guinea pig corneal epithelial cell levels of MMP-9 were increased, and that ALDH3A1 activity (most abundant soluble protein in the cornea, Estey et al., 2007) was increased during the first 18 months and then it decayed. The lipid peroxidation marker malondialdehyde (MDA) (Grotto, 2009) concentration followed the same pattern than ALDH3A1 activity. Moreover, we found that animals fed with deficient AA diet showed more pronounced abnormalities in the cornea and in the crystalline lens (unpublished data). All these findings are compatible with a state of chronic oxidative stress.

It is well known that combination of near continual exposure of the cornea and ocular surface to UVR and molecular oxygen can provoke oxidative stress and tissue damage. Oxidative stress can be defined as an imbalance between reactive oxygen species (ROS) and antioxidants (Cejka and Cejkova, 2015). Among the antioxidants we can mention enzymatic and non-enzymatic molecules. Some of the enzymatic antioxidants are constituted by aldehyde dehydrogenases (ALDHs), catalase, and superoxide dismutase (Chance et al., 1979; Fridovich, 1995; Harrison and Arosio, 1996; Chen et al., 2013), whereas AA, reduced glutathione (GSH), α-tocopherol and NAD(P)H are among the non-enzymatic antioxidants (Dickinson and Forman, 2002; Machlin and Bendich, 1987).

Oxidative stress can cause peroxidation and further damage of lipids, nucleic acids, bases, and proteins. The eye is one of the major targets of the ROS and reactive nitrogen species (RNS) attack due to exposition to several environmental factors like high pressure of oxygen, light, UVR, ionizing radiation, chemical pollutants and pathogenic microbes, which are able to shift the redox status of a cell towards oxidizing conditions. There is increasing evidence indicating that persistent oxidative stress contributes to the development of many ocular diseases such as certain types of keratitis, pterygium, and pinguecula, among others (Kruk et al., 2015).

Our hypothesis for CDK genesis is that individuals with prolonged corneal exposure to multiple unfavorable environmental conditions (e.g., excessive UVR-B exposure, lack of vegetation/shade, dry/windy climate, particle bombardment, AA partial nutritional deficiency, lack of eye protection, genetic factors, etc.) would develop inflammatory processes and oxidative stress leading to progressive degradation and accumulation of proteinaceous material in Bowman's layer and, in advances cases of the disease, in the superficial stroma and deep epithelium (Urrets-Zavalia et al., 2012; Holopainen et al., 2012; Serra et al., 2015).

In the present study, we have determined phospholipids (PC and PS) present in control and CDK affected areas from patients' corneas using triple quadrupole mass spectrometry, in parent-ion and neutral loss scan modes with parameters previously established in the lipid field and widely used for ocular tissue in the study of some ophthalmological diseases (Han et al., 2012; Bhattacharya, 2013; Wang et al., 2016). Phospholipids are the basic building blocks of cell membranes, arranged as bilayer membranes. Membrane phospholipids create a hydrophobic environment for transmembrane protein function and communication. Some membrane lipids are substrates for production of lipid second messengers, which are metabolized by enzymatic activity from phospholipid precursors (Fahy et al., 2011; Aribindi et al., 2013b; Edwards et al., 2014; Li et al., 2015).

Corneal lipid content was studied in humans and animals many years ago (Feldman, 1967; Broekhuyse, 1968; Bazan and Bazan, 1984). Bazan et al. (1984) established that corneal rabbit epithelium has larger phospholipid content and more saturated than in the rest of the cornea. Conversely, corneal endothelium has a higher unsaturation level, according with water permeability of this layer (three times higher than in epithelium). Herein, we report data that clearly shows decreased levels of total phospholipids, PC and PS in the affected CDK epithelium area (in grade 1 as well as grade 2) compared to the non-affected areas. We also describe phospholipids uniquely enriched in control areas, and others only present in CDK affected areas (table 2). At the same time, corneal epithelial cells from CDK grade 1 and grade 2 patients' eyes present a common PC and PS composition (table 3).

It is known that UVR can induce lipid peroxidation in many cell types including human corneal epithelial cells. UVR leads to the production of ROS that initiate lipid peroxidation by attacking the polyunsaturated fatty acids chains in cell membrane phospholipids, and may cause the accumulation of reactive aldehydes. Unlike ROS, aldehydes are generally long-lived compounds that can diffuse through the cell and react with biological targets distant from the site of origin (Estey et al., 2007). Lipid peroxidation has been involved in several disorders such as atherogenesis, neurodegenerative diseases, cataractogenesis, and retinopathy (Awasthi et al., 1996; Witting et al., 1999; Butterfield et al., 2001; Kumar et al., 2001; Totan et al., 2001). Lipid peroxidation as a consequence of oxidative stress may have been taking place in corneas from CDK patients. This could account for the reduction in phospholipid concentrations that was observed.

In summary, we have studied for the first time phospholipid composition in corneal epithelial cells from CDK patients using shotgun lipidomics (direct infusion in triple quadrupole mass spectrometry), and we have found new evidences in favor of our hypothesis

about the etiopathogenesis of CDK. The lower total amount of phospholipids observed in affected areas compared to control areas, and a differential composition between healthy corneal epithelial areas and CDK affected areas, could be signs of an active oxidative stress process occurring in CDK corneas.

Acknowledgments

We thank Yennifer Guerra for assistance with bioinformatic analyses.

This work was partly supported by a grant FONCYT from Argentina, and an unrestricted grant to University of Miami from Research to Prevent Blindness (RPB), NIH grants EY016112 and EY14801, Department of Defense grant W81XWH-15-1-0079.

References

Aribindi K, Guerra Y, Lee RK, Bhattacharya SK. Comparative phospholipid profiles of control and glaucomatous human trabecular meshwork. Invest Ophthalmol Vis Sci. 2013a; 54:3037–3044. [PubMed: 23557733]

Aribindi K, Guerra Y, Piqueras MC, Banta JT, Lee RK, Bhattacharya SK. Cholesterol and glycosphingolipids of human trabecular meshwork and aqueous humor: comparative profiles from control and glaucomatous donors. Curr Eye Res. 2013b; 38:1017–1026. [PubMed: 23790057]

Awasthi S, Srivatava SK, Piper JT, Singhal SS, Chaubey M, Awasthi YC. Curcumin protects against 4-hydroxy-2-transnonenal-induced cataract formation in rat lenses. Am J Clin Nutr. 1996; 64:761–766. [PubMed: 8901798]

Baquis E. Die colloïde Degeneration der Cornea. Ein Beitragzur Kenntniss der Entstehung des Colloïdsausepithelialen Elementen. Albrecht von Graefes Archivfür Ophthalmologie. 1898; 46:553–620.

Bazan HE, Bazan NG. Composition of phospholipids and free fatty acids and incorporation of labeled arachidonic acid in rabbit cornea. Comparison of epithelium, stroma and endothelium. Curr Eye Res. 1984; 3:1313–1319. [PubMed: 6439475]

Bhattacharya SK. Recent advances in shotgun lipidomics and their implication for vision research and ophthalmology. Curr Eye Res. 2013; 38:417–427. [PubMed: 23330842]

Bradford MM. A rapid and sensitive method for the quantitation of microgram quantities of protein utilizing the principle of protein-dye binding. Anal Biochem. 1976; 72:248–254. [PubMed: 942051]

Broekhuyse RM. Phospholipids in tissues of the eye. Isolation, characterization and quantitative analysis by two dimensional thin-layer chromatography of diacyl and vinyl-ether phospholipids. Biochim Biophys Acta. 1968; 152:307–315. [PubMed: 4296335]

Butterfield DA, Drake J, Pocernich C, Castegna A. Evidence ofoxidative damage in Alzheimer's disease brain: central role for amyloidbeta-peptide. Trends Mol Med. 2001; 7:548–554. [PubMed: 11733217]

Cejka C, Cejkova J. Oxidative stress to the cornea, changes in corneal optical properties, and advances in treatment of corneal oxidative injuries. Oxid Med Cell Longev. 2015; 591530 2015. Review. doi: 10.1155/2015/591530

Chance B, Sies H, Boveris A. Hydroperoxide metabolism in mammalian organs. Physiol Rev. 1979; 59:527–605. [PubMed: 37532]

Checa A, Bedia C, Jaumot J. Lipidomic data analysis: tutorial, practical guidelines and applications. Anal Chim Acta. 2015; 885:1–16. [PubMed: 26231889]

Chen Y, Thompson DC, Koppaka V, Jester JV, Vasiliou V. Ocular aldehyde dehydrogenases: protection against ultraviolet damage and maintenance oftransparency for vision. Prog Retin Eye Res. 2013; 33:28–39. [PubMed: 23098688]

Dickinson DA, Forman HJ. Glutathione in defense and signaling: lessons from a small thiol. Ann NY Acad Sci. 2002; 973:488–504. [PubMed: 12485918]

Edwards G, Aribindi K, Guerra Y, Bhattacharya SK. Sphingolipids and ceramides of mouse aqueous humor: Comparative profiles from normotensive and hypertensive DBA/2J mice. Biochimie. 2014; 105:99–109. [PubMed: 25014247]

Edwards G, Aribindi K, Guerra Y, Lee RK, Bhattacharya SK. Phospholipid profiles of control and glaucomatous human aqueous humor. Biochimie. 2014; 101:232–247. [PubMed: 24561385]

Enriquez-Algeciras M, Bhattacharya SK. Lipidomic mass spectrometry and its application in neuroscience. World J Biol Chem. 2013; 4:102–110. [PubMed: 24340133]

Estey T, Piatigorsky J, Lassen N, Vasiliou V. ALDH3A1: a corneal crystalline with diverse functions. Exp Eye Res. 2007; 84:3–12. [PubMed: 16797007]

Fahy E, Subramaniam S, Murphy RC, et al. Update of the LIPID MAPS comprehensive classification system for lipids. J Lipid Res. 2009; 50:S9–S14. [PubMed: 19098281]

Fahy E, Cotter D, Sud M, Subramaniam S. Lipid classification, structures and tools. Biochim Biophys Acta. 2011; 1811:637–647. [PubMed: 21704189]

Feldman GL. Human ocular lipids: Their analysis and distribution. Surv Ophthalmol E. 1967:207–243.

Freedman A. Labrador keratopathy. Arch Ophthalmol. 1965; 74:198–202. [PubMed: 14318495]

Fridovich I. Superoxide radical and superoxide dismutases. Annu Rev Biochem. 1995; 64:97–112. [PubMed: 7574505]

Fujishima H, Fukagawa K, Okada N, et al. Chemotactic responses of peripheral blood eosinophils to prostaglandin D2 in atopic keratoconjunctivitis. Ann Allergy Asthma Immunol. 2013; 111:126–131. [PubMed: 23886231]

Gray RH, Johnson GJ, Freedman A. Climatic droplet keratopathy. Surv Ophthalmol. 1992; 36:241–253. Review. [PubMed: 1549808]

Grotto D. Importance of the lipid peroxidation biomarkers and methodological aspects for malondialdehyde quantification. Quím Nova. 2009; 32:169–174. online.

Ham BM, Jacob JT, Keese MM, Cole RB. Identification, quantification and comparison of major non-polar lipids in normal and dry eye tear lipidomes by electrospray tandem mass spectrometry. J Mass Spectrom. 2004; 39:1321–1336. [PubMed: 15532045]

Han X, Yang K, Gross RW. Multi-dimensional mass spectrometry-based shotgunlipidomics and novel strategies for lipidomic analyses. Mass Spectrom Rev. 2012; 31:134–178. [PubMed: 21755525]

Harrison PM, Arosio P. The ferritins: molecular properties, iron storage function and cellular regulation. Biochim Biophys Acta. 1275:1996. 161–203.

Holopainen JM, Robciuc A, Cafaro TA, et al. Pro inflammatory cytokines and gelatinasesin climatic droplet keratopathy. Invest Ophthalmol Vis Sci. 2012; 53:3527–3535. [PubMed: 22570354]

Holopainen JM, Serra HM, Sánchez MC, et al. Altered expression of matrix metalloproteinases and their tissue inhibitors as possible contributors to corneal droplet formation in climatic droplet keratopathy. Acta Ophthalmol. 2011; 89:569–574. [PubMed: 19900203]

Iverson SJ, Lang SL, Cooper MH. Comparison of the Bligh and Dyer and Folch methods for total lipid determination in a broad range of marine tissue. Lipids. 2001; 36:1283–1287. [PubMed: 11795862]

Kaji Y, Nagai R, Amano S, et al. Advanced glycation end product deposits in climatic droplet keratopathy. Br J Ophthalmol. 2007; 91:85–88. [PubMed: 16973666]

Kaji Y, Oshika T, Takazawa Y, et al. Accumulation of D-beta-aspartic acid-containing proteins in age-related ocular diseases. Chem Biodivers. 2010; 7:1364–1370. [PubMed: 20564555]

Kruk J, Kubasik-Kladna K, Aboul-Enein HY. The role of oxidative stress in the pathogenesis of eye diseases: current status and a dual role of physicalactivity. Mini Rev Med Chem. 2015; 16:241–257. [PubMed: 26586128]

Kumar RS, Anthrayose CV, Iyer KV, Vimala B, Shashidhar S. Lipid peroxidation and diabetic retinopathy. Indian J Med Sci. 2001; 55:133–138. [PubMed: 11482166]

Li J, Wang X, Zhang T, et al. A review on phospholipids and their main applications in drug delivery systems. Asian J of Pharmaceutical Sci. 2015; 10:81–98.

Liliom K, Guan Z, Tseng JL, Desiderio DM, Tigyi G, Watsky MA. Growthfactor-like phospholipids generated after corneal injury. Am J Physiol. 1998; 274:1065–1074.

Machlin LJ, Bendich A. Free radical tissue damage: protective role ofantioxidant nutrients. FASEB J. 1987; 1:441–445. [PubMed: 3315807]

Menegay M, Lee D, Tabbara KF, et al. Proteomic analysis of climatic keratopathy droplets. Invest Ophthalmol Vis Sci. 2008; 49:2829–2837. [PubMed: 18378572]

Rantamäki AH, Seppänen-Laakso T, Oresic M, Jauhiainen M, Holopainen JM. Human tear fluid lipidome: from composition to function. PLoS One. 2011; 6:e19553. [PubMed: 21573170]

Robciuc A, Rantamäki AH, Jauhiainen M, Holopainen JM. Lipid-modifying enzymes in human tear fluid and corneal epithelial stress response. Invest Ophthalmol Vis Sci. 2014; 55:16–24. [PubMed: 24302584]

Serra HM, Holopainen JM, Beuerman R, Kaarniranta K, Suarez MF, Urrets-Zavalia JA. Climatic droplet keratopathy: an old disease in new clothes. Acta Ophthalmol. 2015; 93:496–504. [PubMed: 25626588]

Suarez MF, Correa L, Crim N, et al. Climatic droplet keratopathyin Argentina: involvement of environmental agents in its genesis which would open the prospect for new therapeutic interventions. Biomed Res Int. 2015; 527835 2015.

Tabbara KF. Climatic droplet keratopathy. Int Ophthalmol Clin. 1986; 26:63–68.

Totan Y, Cekic O, Borazan M, Uz E, Sogut S, Akyol O. Plasmamalondialdehyde and nitric oxide levels in age related macular degeneration. Br J Ophthalmol. 2001; 85:1426–1428. [PubMed: 11734513]

Urrets-Zavalia JA, Croxatto JO, Holopainen JM, et al. In vivo confocal microscopy study of climatic droplet keratopathy. Eye (Lond). 2012; 26:1021–1023. [PubMed: 22538217]

Urrets-Zavalía JA, Maccio JP, Knoll EG, Cafaro TA, Urrets-Zavalía EA, Serra HM. Surface alterations, corneal hypoesthesia and iris atrophy in patients with climatic droplet keratopathy. Cornea. 2007; 26:800–804. [PubMed: 17667612]

Wang M, Wang C, Han RH, Han X. Novel advances in shotgun lipidomicsforbiology and medicine. Prog Lipid Res. 2016; 61:83–108. [PubMed: 26703190]

Witting PK, Pettersson K, Ostlund-Lindqvist AM, Westerlund C, Eriksson AW, Stocker R. Inhibition by a coantioxidant of aortic lipoprotein lipid peroxidation and atherosclerosis in apolipoprotein E and low density lipoprotein receptor gene double knockout mice. FASEB J. 1999; 13:667–675. [PubMed: 10094927]

Yang K, Han X. Lipidomics: Techniques, Applications, and Outcomes Related to Biomedical Sciences. Trends Biochem Sci. 2016; 41:954–969. [PubMed: 27663237]

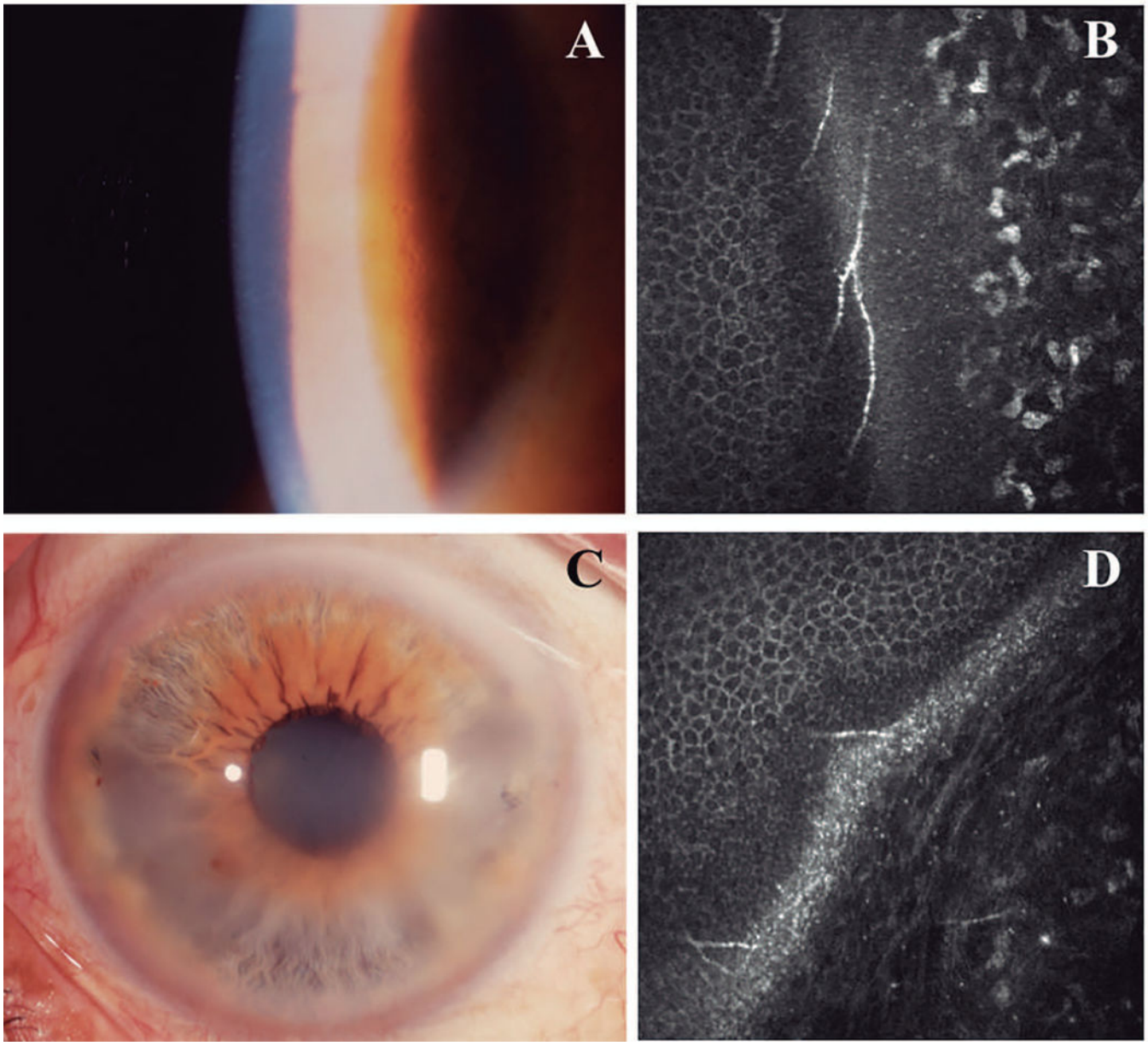

Figure 1.

Slit-lamp images of corneas in two CDK patients (**A** and **C**), and *in vivo* confocal microscopy (**B** and **D**). Grade 1 disease with peripheral nasal haziness (A) and grade 2 with diffuse haziness affecting also the central cornea (C), caused by tiny droplets of different sizes visualized with magnification and back-scattered slit-illumination. CDK grade 1 presents dot-like deposits at the level of Bowman's layer and (**B**), and CDK grade 2 shows an increase in the density of the hyperreflective dot-like deposits in Bowman's layer and superficial stroma (**D**).

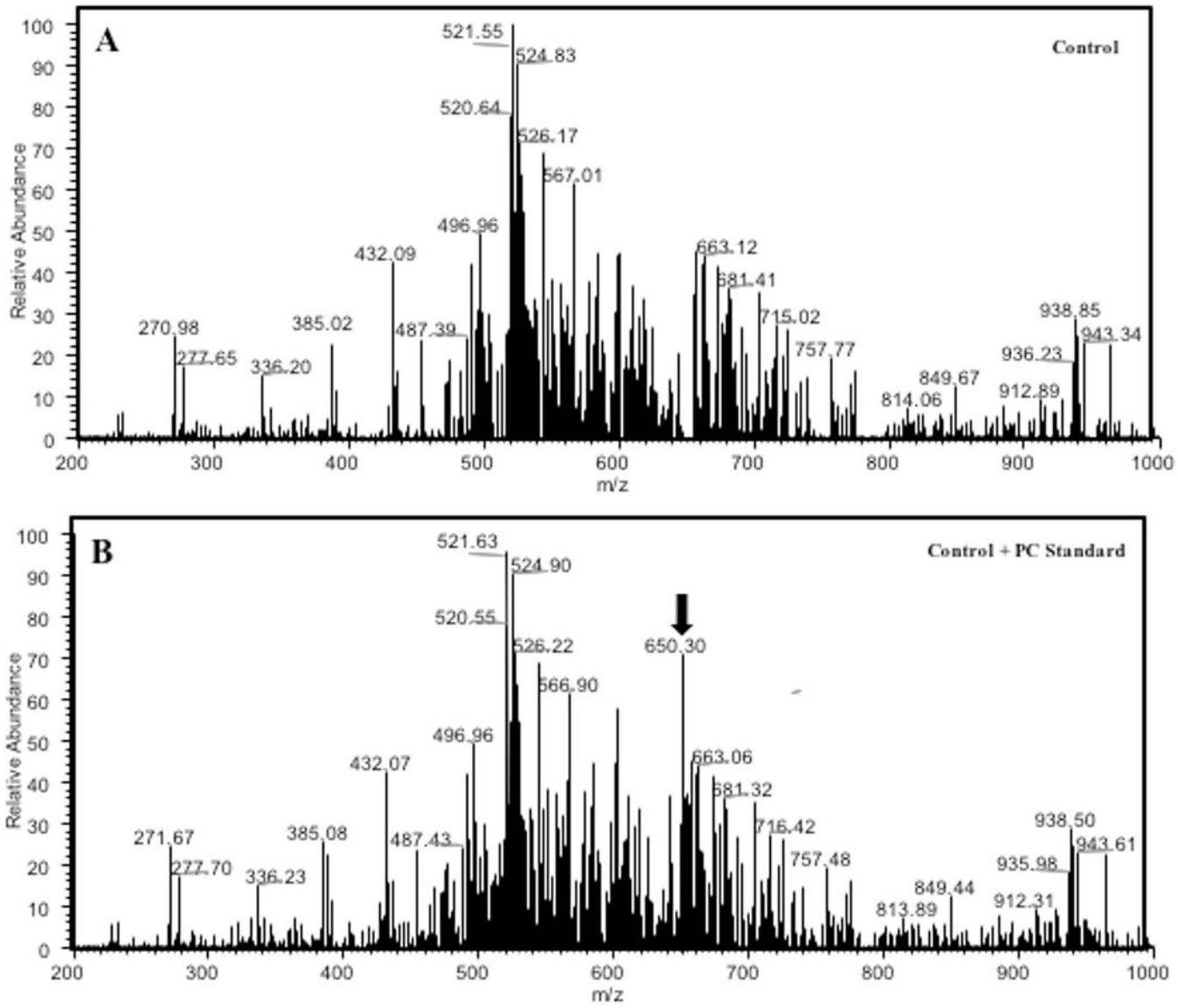

Figure 2.

Representative electro spray ionization tandem mass spectrometric analysis of PC lipid class extracted from CDK human corneal epithelium control area, in positive ion mode. (**A**) A parent ion scan (PIS) scanning of m/z =184.0 for PC class. (**B**) Representative PIS as presented above with internal standard addition (arrow; m/z= 650.3, 10pmol) to perform ratiometric quantification of all identified lipids in PC class.

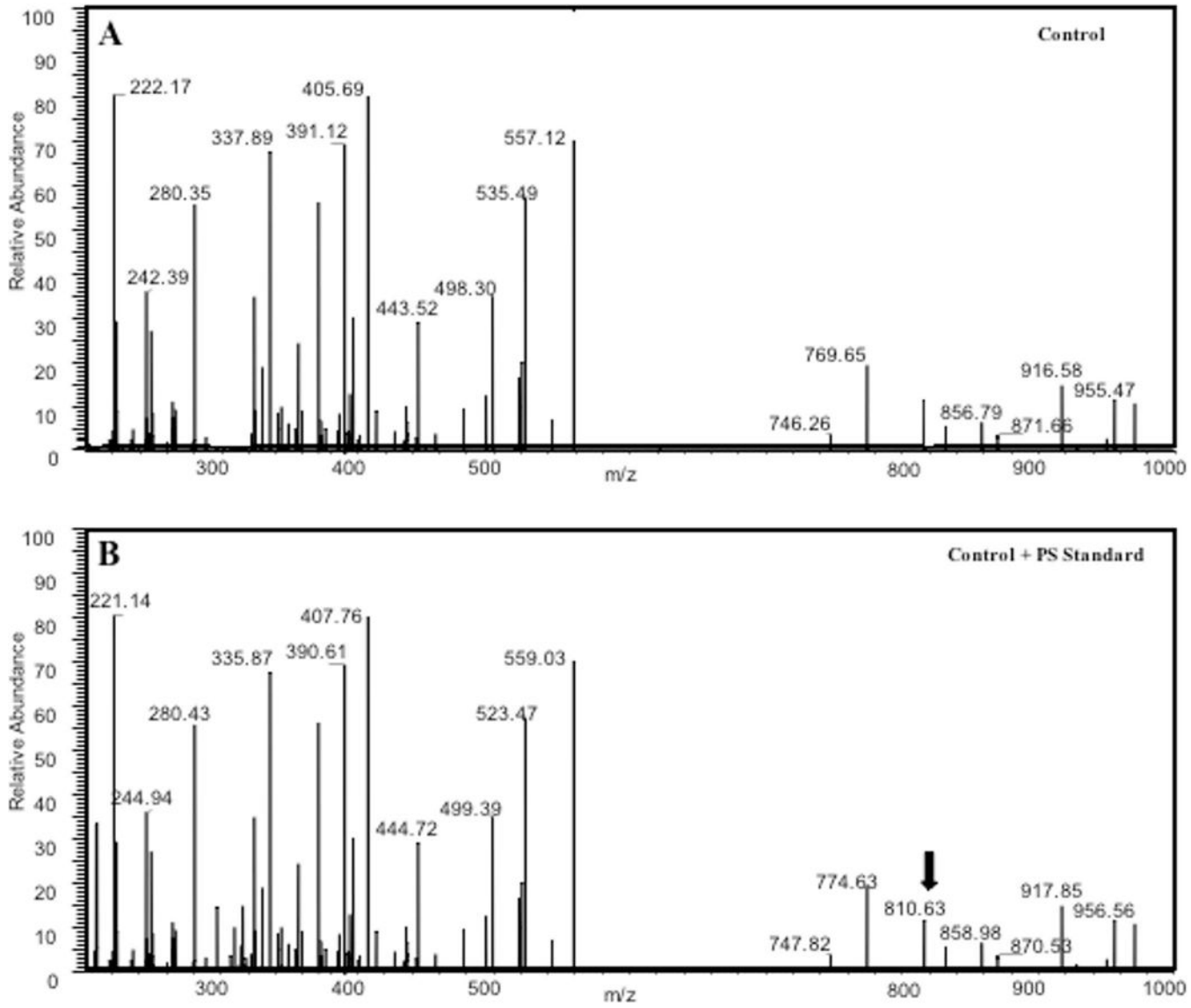

Figure 3.

Representative electro spray ionization tandem mass spectrometric analysis of PS lipid class extracted from CDK human corneal epithelium control area, in neutral loss scan (NLS). (**A**) NLS scanning of m/z =87.1 for PS class. (**B**) Representative NLS as presented above with internal standard addition (arrow; m/z= 810.63, 10pmol) to perform ratiometric quantification of all identified lipids in PS class.

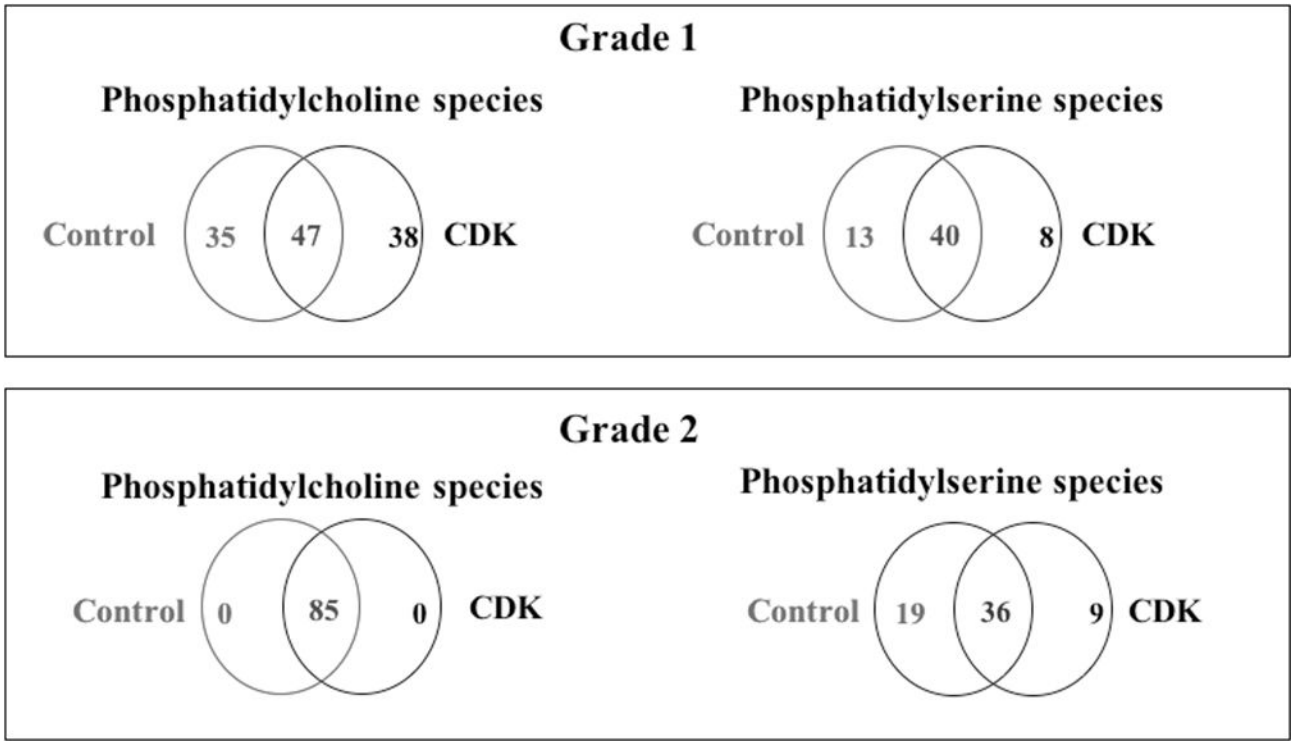

Figure 4.

Venn diagram showing common and unique lipid species found in control areas and CDK affected areas, for CDK grade 1 (superior panel) and CDK grade 2 (inferior panel), for PC and PS. Diagram intersections' show common lipids between control and affected areas.

Table 1

Total average protein normalized phosphatidylcholine and phosphatidylserine in the CDK corneal specimens.

Patient / CDK grade	*Phosphatidylcholines (pmol/μg protein)*		*Phosphatidylserines (pmol/μg protein)*		*Total phospholipids amount (pmol/μg protein)*	
	Control	*CDK*	*Control*	*CDK*	*Control*	*CDK*
Grade 1	11792.35	2510.78	29936.93	2981.93	**41729.28**	**5492.71**
Grade 2	2583.76	450.44	489172.16	13572.31	**491755.92**	**14022.75**

Table 2

Unique phospholipid species identified in control and CDK affected areas.

	m/z*	Amount, pmol per Species/μg protein	LIPIDMAPS ID
Phosphatydilcholines			
Grade 1			
Control			
PC(6:2(2E,4E)/6:2(2E,4E))	449.5343475	35.10504116	LMGP01011235
PC(6:0/6:0)	461.611969	60.97552036	LMGP01011229
PC(8:2(2E,4E)/8:2(2E,4E))	508.7760621	336.7085264	LMGP01011254
PC(O-16:0/2:0)	532.708313	30.49454999	LMGP01020046
PC(22:6(4Z,7Z,10Z,13Z,16Z,19Z)/0:0)	576.223999	27.63661101	LMGP01050056
PC(12:0/14:1(9Z))	653.0681152	188.8764232	LMGP01011316
PC(18:0/11:1(10E))	697.8502197	123.003872	LMGP01010735
PC(12:0/18:4(6Z,9Z,12Z,15Z))	705.4578247	16.83355497	LMGP01011326
PC(13:0/18:4(6Z,9Z,12Z,15Z))	719.3928223	261.6877919	LMGP01011351
PC(14:0/18:4(6Z,9Z,12Z,15Z))	734.7036133	33.99468733	LMGP01010499
PC(14:0/18:3(9Z,12Z,15Z))	736.7713623	139.3388865	LMGP01010497
PC(O-16:0/17:2(9Z,12Z))	739.5371704	10.7416212	LMGP01020184
PC(10:0/22:0)	743.0431061	95.55680672	LMGP01010397
PC(14:0/20:5(5Z,8Z,11Z,14Z,17Z))	760.842041	14.79965082	LMGP01010508
PC(14:0/20:4(5Z,8Z,11Z,14Z))	761.8012695	11.29438532	LMGP01010506
PC(16:0/18:3(6Z,9Z,12Z))	764.8153687	16.84177156	LMGP01010598
PC(13:0/22:2(13Z,16Z))	780.9053548	141.4017152	LMGP01011360
PC(18:0/18:2(10Z,12Z))	793.9078979	4.870731935	LMGP01010764
PC(15:1(9Z)/22:4(7Z,10Z,13Z,16Z))	802.3403931	0.292454956	LMGP01011460
PC(16:0/22:6(4E,7E,10E,13E,16E,19E))	814.689621	35.41917971	LMGP01010650
PC(16:0/22:4(7Z,10Z,13Z,16Z))	818.5667572	35.02464907	LMGP01010642
PC(18:0/20:2(11Z,14Z))	822.8417358	3.113532506	LMGP01010788
PC(17:0/22:6(4Z,7Z,10Z,13Z,16Z,19Z))	829.2927246	19.62032538	LMGP01010720
PC(18:0/22:3(10Z,13Z,16Z))	848.0913086	10.55761574	LMGP01010812
PC(20:5(5Z,8Z,11Z,14Z,17Z)/22:5(7Z,10Z,13Z,16Z,19Z))	861.9257813	12.02594653	LMGP01011058
PC(20:3(8Z,11Z,14Z)/22:6(4Z,7Z,10Z,13Z,16Z,19Z))	864.4815369	96.29052353	LMGP01011896
PC(20:1(11Z)/22:6(4Z,7Z,10Z,13Z,16Z,19Z))	869.3223114	4.978646959	LMGP01011834
PC(23:0/18:0)	869.6445313	9.01741973	LMGP01011130
PC(20:0/22:6(4Z,7Z,10Z,13Z,16Z,19Z))	870.8692932	18.18734822	LMGP01011028
PC(20:0/22:5(7Z,10Z,13Z,16Z,19Z))	871.7922363	63.0557569	LMGP01011027
PC(20:1(11Z)/22:2(13Z,16Z))	877.6144409	0.34022481	LMGP01011832
PC(22:4(7Z,10Z,13Z,16Z)/22:6(4Z,7Z,10Z,13Z,16Z,19Z))	890.7302246	10.41447043	LMGP01012096
PC(22:1(11Z)/22:6(4Z,7Z,10Z,13Z,16Z,19Z))	897.191803	58.34030765	LMGP01012034
PC(22:1(11Z)/22:2(13Z,16Z))	905.4731445	11.1785486	LMGP01012032
PC(20:0/24:1(15Z))	908.4393921	55.37025535	LMGP01011032
CDK			

	m/z*	Amount, pmol per Species/μg protein	LIPIDMAPS ID
PC(P-15:0/0:0)	475.3136597	2.258060045	LMGP01070003
PC(0:0/14:0)	475.7080078	8.760073598	LMGP01050073
PC(17:2(9Z,12Z)/0:0)	512.0413666	139.3999566	LMGP01050127
PC(20:3(8Z,11Z,14Z)/0:0)	555.0397949	9.151008296	LMGP01050133
PC(10:0/10:0)	574.9521484	58.01008602	LMGP01010380
PC(16:0/9:0(COOH))	674.8492432	43.25367692	LMGP20010007
PC(12:0/17:2(9Z,12Z))	695.5105082	59.84938759	LMGP01011322
PC(12:0/18:3(6Z,9Z,12Z))	709.3492432	29.40629858	LMGP01011324
PC(13:0/18:3(6Z,9Z,12Z))	722.7244721	23.22549354	LMGP01011349
PC(14:0/18:2(11Z,14Z))	738.9689941	9.61773106	LMGP01010494
PC(14:0/18:1(11Z))	740.4227498	10.14359376	LMGP01010490
PC(13:0/20:3(8Z,11Z,14Z))	751.0203247	6.071596573	LMGP01011355
PC(15:0/18:1(11Z))	754.4980469	16.34204123	LMGP01010541
PC(10:0/23:0)	757.4887085	7.0248453	LMGP01010399
PC(16:0/18:2(10E,12Z))	765.9030151	19.37539039	LMGP01010585
PC(16:0/18:1(9Z))	767.6375427	5.401143878	LMGP01010005
PC(18:2(9Z,12E)/17:2(9Z,11E))	777.0445557	8.175188459	LMGP01010931
PC(14:0/22:6(4Z,7Z,10Z,13Z,16Z,19Z))	787.3533936	8.379876858	LMGP01010512
PC(16:0/20:5(5Z,8Z,11Z,14Z,17Z))	789.5361938	5.682940604	LMGP01010633
PC(18:0/18:1(11Z))	797.3813477	1.802717735	LMGP01010750
PC(16:1(9Z)/22:6(4Z,7Z,10Z,13Z,16Z,19Z))	812.9232788	5.572865494	LMGP01010696
PC(17:2(9Z,12Z)/22:6(4Z,7Z,10Z,13Z,16Z,19Z))	823.7950745	5.964470179	LMGP01011580
PC(18:3(6Z,9Z,12Z)/22:6(4Z,7Z,10Z,13Z,16Z,19Z))	836.2522125	8.435849515	LMGP01011670
PC(18:2(9Z,12Z)/22:6(4Z,7Z,10Z,13Z,16Z,19Z))	838.1468811	2.276002421	LMGP01010947
PC(18:0/22:6(4Z,7Z,10Z,13Z,16Z,19Z))	842.451416	5.65016685	LMGP01010821
PC(18:0/22:5(4Z,7Z,10Z,13Z,16Z))	844.7405396	0.22199696	LMGP01010816
PC(16:0/24:1(15Z))	852.4516602	0.506300409	LMGP01010659
PC(19:1(9Z)/22:6(4Z,7Z,10Z,13Z,16Z,19Z))	854.8773652	7.943575465	LMGP01011786
PC(19:0/22:6(4Z,7Z,10Z,13Z,16Z,19Z))	857.3092651	0.602203978	LMGP01011755
PC(19:1(9Z)/22:4(7Z,10Z,13Z,16Z))	858.6088867	0.439391289	LMGP01011785
PC(16:0/26:2(5Z,9Z))	878.7354736	7.857161887	LMGP01010665
PC(16:0/26:0)	882.1089478	3.17402956	LMGP01010663
PC(22:0/22:6(4Z,7Z,10Z,13Z,16Z,19Z))	899.3740845	6.28295672	LMGP01012003
PC(22:1(11Z)/22:4(7Z,10Z,13Z,16Z))	900.31604	4.064865082	LMGP01012033
PC(22:0/22:4(7Z,10Z,13Z,16Z))	902.128006	12.31269729	LMGP01012002
PC(22:1(13E)/22:1(13E))	906.6358643	8.243314415	LMGP01011108
PC(18:0/26:0)	910.7911377	23.81364481	LMGP01010828
PC(20:0/26:0)	938.448761	5.159413759	LMGP01011034
Phosphatydilserines			
Grade 1			
Control			
PS(15:0/0:0)	486.2679443	349.4908061	LMGP03050031

	m/z*	Amount, pmol per Species/μg protein	LIPIDMAPS ID
PS(16:1(9Z)/0:0)	490.930191	1351.894279	LMGP03050010
PS(18:0/0:0)	530.1671143	456.3458717	LMGP03050006
PS(20:0/0:0)	554.648584	684.5651013	LMGP03050012
PS(22:0/0:0)	585.0875854	179.8953782	LMGP03050025
PS(14:1(9Z)/14:1(9Z))	670.7094727	32.97216305	LMGP03010919
PS(12:0/22:2(13Z,16Z))	756.0275879	97.04654863	LMGP03010066
PS(13:0/22:2(13Z,16Z))	769.5744629	191.1471607	LMGP03010090
PS(18:0/18:1(9Z))	792.4706421	41.71102472	LMGP03010025
PS(17:0/22:2(13Z,16Z))	826.5164795	394.1171434	LMGP03010246
PS(17:0/22:1(11Z))	826.6235962	173.221204	LMGP03010245
PS(19:0/22:2(13Z,16Z))	853.6619873	434.259899	LMGP03010477
PS(22:0/22:2(13Z,16Z))	894.7367554	5.440477649	LMGP03010723
CDK			
PS(22:1(11Z)/0:0)	580.0860748	33.72772797	LMGP03050023
PS(12:0/16:1(9Z))	673.6097412	6.176727075	LMGP03010049
PS(12:0/20:2(11Z,14Z))	728.3601685	57.60975185	LMGP03010060
PS(13:0/22:4(7Z,10Z,13Z,16Z))	766.5620728	2.502793177	LMGP03010091
PS(18:1(9Z)/22:6(4Z,7Z,10Z,13Z,16Z,19Z))	829.5198975	4.677840797	LMGP03010045
PS(19:0/21:0)	852.2431335	50.02072802	LMGP03010474
PS(20:0/22:2(13Z,16Z))	868.54953	7.575445338	LMGP03010526
PS(21:0/22:0)	890.7318624	57.13378798	LMGP03010698
Grade 2			
Control			
PS(12:0/0:0)	439.9199524	20160.19245	LMGP03050008
PS(16:1(9Z)/0:0)	492.0351257	16760.19337	LMGP03050010
PS(19:1(9Z)/0:0)	535.6446533	38229.62984	LMGP03050019
PS(22:4(7Z,10Z,13Z,16Z)/0:0)	575.9509277	5370.664303	LMGP03050014
PS(22:0/0:0)	584.8668213	399.0301165	LMGP03050025
PS(12:0/13:0)	639.6738281	1485.057448	LMGP03010001
PS(14:0/12:0)	655.169632	2134.979121	LMGP03010931
PS(12:0/15:1(9Z))	658.8825073	1073.721191	LMGP03010048
PS(14:1(9Z)/14:1(9Z))	672.0128784	5326.561203	LMGP03010919
PS(14:0/14:0)	681.993866	1454.833471	LMGP03010028
PS(13:0/18:2(9Z,12Z))	713.6038208	1105.076469	LMGP03010078
PS(12:0/20:2(11Z,14Z))	727.508667	1256.958181	LMGP03010060
PS(12:0/22:2(13Z,16Z))	754.8304749	664.3245694	LMGP03010066
PS(13:0/22:4(7Z,10Z,13Z,16Z))	767.3230438	4198.550223	LMGP03010091
PS(17:0/21:0)	824.0448914	1161.380728	LMGP03010243
PS(17:0/22:1(11Z))	827.3017273	109.6109416	LMGP03010245
PS(19:0/22:2(13Z,16Z))	853.5385742	42064.46901	LMGP03010477
PS(20:0/22:2(13Z,16Z))	867.8551636	711.0927161	LMGP03010526
PS(22:6(4Z,7Z,10Z,13Z,16Z,19Z)/22:6(4Z,7Z,10Z,13Z,16Z,19Z))	877.0893402	1496.288525	LMGP01030017

	m/z*	Amount, pmol per Species/μg protein	LIPIDMAPS ID
CDK			
PS(18:2(9Z,12Z)/0:0)	517.1746216	44.51834435	LMGP03050011
PS(18:0/0:0)	529.024292	152.087076	LMGP03050006
PS(12:0/16:1(9Z))	674.1259766	2.737743873	LMGP03010049
PS(13:0/18:3(6Z,9Z,12Z))	711.3513184	24.13983471	LMGP03010079
PS(16:0/22:6(4Z,7Z,10Z,13Z,16Z,19Z))	805.9547729	13.41827269	LMGP03010043
PS(18:0/20:4(5Z,8Z,11Z,14Z))	815.3720093	125.3012959	LMGP03010039
PS(17:0/22:2(13Z,16Z))	826.2357788	277.8600108	LMGP03010246
PS(19:0/22:0)	863.70578	25.48655768	LMGP03010475
PS(22:4(7Z,10Z,13Z,16Z)/22:6(4Z,7Z,10Z,13Z,16Z,19Z))	887.5043945	106.6639534	LMGP01030018

Table 3

Common phospholipid species identified in both, control and CDK affected areas.

	m/z*	Amount, pmol per Species/μg protein	LIPIDMAPS ID
Phosphatydilcholines			
Grade 1			
PC(2:0/0:0)	294.646521	119.0274412	LMGP01050043
PC(0:0/3:1(2E))	312.3085632	0.955340492	LMGP01050088
PC(0:0/4:0)	328.5174103	171.4947089	LMGP01050089
PC(2:0/2:0)	345.2589264	25.29684283	LMGP01010992
PC(6:0/0:0)	360.7000733	85.34025255	LMGP01050062
PC(3:0/3:0)	373.3088633	158.4236004	LMGP01011215
PC(8:0/0:0)	390.3349152	28.19330422	LMGP01050066
PC(O-10:1(9E)/0:0)	399.1379204	50.14397867	LMGP01060027
PC(10:0/0:0)	414.0388184	168.5467928	LMGP01050005
PC(5:0/5:0)	430.6288147	301.5102334	LMGP01011225
PC(12:0/0:0)	442.1364975	41.97399351	LMGP01050009
PC(O-11:1(10E)/2:0)	458.1137187	142.0015605	LMGP01020146
PC(14:1(9Z)/0:0)	468.9347534	134.0907124	LMGP01050014
PC(15:1(9Z)/0:0)	482.7285462	316.4143978	LMGP01050125
PC(16:1(9Z)/0:0)	498.2089463	308.5061021	LMGP01050022
PC(18:4(9E,11E,13E,15E)/0:0)	520.5874023	1156.005517	LMGP01050040
PC(18:3(6Z,9Z,12Z)/0:0)	525.5578613	188.3306353	LMGP01050128
PC(19:3(10Z,13Z,16Z)/0:0)	537.7588501	1.693566016	LMGP01050003
PC(16:1(9Z)/2:0)	542.2512207	69.99420119	LMGP01010693
PC(20:5(5Z,8Z,11Z,14Z,17Z)/0:0)	549.6884155	496.3744142	LMGP01050050
PC(20:2(11Z,14Z)/0:0)	555.9118652	328.6174258	LMGP01050132
PC(6:2(3E,5E)/14:2(11E,13E))	563.8403321	95.79849495	LMGP01011236
PC(18:1(9E)/2:0)	569.2772339	861.9458746	LMGP01010878
PC(22:4(7Z,10Z,13Z,16Z)/0:0)	579.3897247	264.4194871	LMGP01050124
PC(22:2(13Z,16Z)/0:0)	582.6686401	34.07005381	LMGP01050135
PC(18:1(9Z)/4:0)	598.3166504	305.8745425	LMGP01010916
PC(24:0/0:0)	611.7825394	475.51746	LMGP01050057
PC(12:0/12:0)	624.421875	311.3969386	LMGP01010429
PC(12:0/13:0)	643.6590983	463.2832235	LMGP01010001
PC(12:0/15:1(9Z))	664.0793991	841.602332	LMGP01011318
PC(10:0/18:2(9Z,12Z))	677.8133087	689.7408956	LMGP01010393
PC(10:0/18:1(9Z))	684.8070069	220.5491298	LMGP01010392
PC(10:0/18:0)	686.6455383	54.59223528	LMGP01010390
PC(12:0/18:1(9Z))	712.737854	17.62268556	LMGP01010440
PC(10:0/21:0)	728.0479736	2.847456952	LMGP01010396
PC(12:0/20:5(5Z,8Z,11Z,14Z,17Z))	732.6423645	98.46496859	LMGP01011333
PC(13:0/20:5(5Z,8Z,11Z,14Z,17Z))	747.0627747	22.27042735	LMGP01011357

	m/z*	Amount, pmol per Species/μg protein	LIPIDMAPS ID
PC(13:0/20:4(5Z,8Z,11Z,14Z))	749.2914124	41.31325122	LMGP01011356
PC(15:1(9Z)/22:6(4Z,7Z,10Z,13Z,16Z,19Z))	799.3400269	16.9228596	LMGP01011461
PC(17:0/20:4(5Z,8Z,11Z,14Z))	804.3778992	54.65130021	LMGP01010003
PC(17:1(9Z)/22:6(4Z,7Z,10Z,13Z,16Z,19Z))	826.1033936	17.78568203	LMGP01011550
PC(16:0/23:5(8E,11E,14E,17E,20E))	830.2391357	8.993563427	LMGP01010656
PC(22:6(4Z,7Z,10Z,13Z,16Z,19Z)/22:6(4Z,7Z,10Z,13Z,16Z,19Z))	886.4762269	41.85462361	LMGP01011119
PC(23:1(9Z)/23:1(9Z))	927.0930237	134.2862697	LMGP01011141
PC(24:1(15Z)/24:1(15Z))	952.9333598	203.7302272	LMGP01011163
PC(22:0/26:0)	965.081604	37.28316211	LMGP01011107
PC(34:0/16:0)	984.7036705	51.08762534	LMGP01011218
Grade 2			
PC(2:0/0:0)	300.7475204	3.981478114	LMGP01050043
PC(0:0/3:1(2E))	316.1439412	25.57478466	LMGP01050088
PC(0:0/4:0)	330.2403361	2.286290765	LMGP01050089
PC(2:0/2:0)	343.6709595	22.23310934	LMGP01010992
PC(6:0/0:0)	358.9837341	95.66402265	LMGP01050062
PC(3:0/3:0)	370.5003433	195.937209	LMGP01011215
PC(8:0/0:0)	391.1658936	0.226786815	LMGP01050066
PC(O-10:1(9E)/0:0)	397.5191345	3.512329217	LMGP01060027
PC(4:0/4:0)	406.9981689	15.65223013	LMGP01011222
PC(10:0/0:0)	416.5296326	196.4323143	LMGP01050005
PC(5:0/5:0)	429.5228831	23.91039676	LMGP01011225
PC(12:0/0:0)	440.451149	8.562903876	LMGP01050009
PC(6:2(2E,4E)/6:2(2E,4E))	451.0426025	1.262407207	LMGP01011235
PC(O-11:1(10E)/2:0)	459.2329407	2.376642324	LMGP01020146
PC(14:1(9Z)/0:0)	470.2901306	0.666841011	LMGP01050014
PC(15:1(9Z)/0:0)	484.2517853	117.2943671	LMGP01050125
PC(16:1(9Z)/0:0)	497.7138443	0.415454367	LMGP01050022
PC(O-14:0/2:0)	504.4213715	0.191977505	LMGP01020019
PC(O-17:0/0:0)	505.3683929	135.6667898	LMGP01060013
PC(8:2(2E,4E)/8:2(2E,4E))	509.2782364	9.147315957	LMGP01011254
PC(17:2(9Z,12Z)/0:0)	514.7207642	145.624321	LMGP01050127
PC(17:1(9Z)/0:0)	516.0500488	173.0182473	LMGP01050126
PC(18:3(6Z,9Z,12Z)/0:0)	525.7462158	210.0639731	LMGP01050128
PC(0:0/18:1(9Z))	529.6395264	44.11870543	LMGP01050082
PC(O-16:0/2:0)	531.8207397	0.202057957	LMGP01020046
PC(19:3(10Z,13Z,16Z)/0:0)	538.7858124	1.225915616	LMGP01050003
PC(16:1(9Z)/2:0)	542.2966309	2.055870035	LMGP01010693
PC(20:5(5Z,8Z,11Z,14Z,17Z)/0:0)	549.8468933	1.663656827	LMGP01050050
PC(6:2(3E,5E)/14:2(11E,13E))	562.7392883	129.1237968	LMGP01011236
PC(18:1(9E)/2:0)	570.3476563	3.703695673	LMGP01010878
PC(22:4(7Z,10Z,13Z,16Z)/0:0)	580.1956787	21.28910443	LMGP01050124

	m/z*	Amount, pmol per Species/μg protein	LIPIDMAPS ID
PC(16:0/5:1(4E))	586.2541809	9.473000368	LMGP01010673
PC(18:1(9Z)/4:0)	601.3341064	0.548999836	LMGP01010916
PC(24:0/0:0)	610.3458252	48.39189195	LMGP01050057
PC(12:0/12:0)	620.5292664	69.65722502	LMGP01010429
PC(12:0/13:0)	638.8419088	83.83930245	LMGP01010001
PC(12:0/14:1(9Z))	645.7624207	0.657894935	LMGP01011316
PC(12:0/15:1(9Z))	664.4971771	3.292237794	LMGP01011318
PC(10:0/18:2(9Z,12Z))	677.1966705	128.2524298	LMGP01010393
PC(10:0/18:0)	685.7401123	96.26273872	LMGP01010390
PC(12:0/17:2(9Z,12Z))	691.0081787	2.483937833	LMGP01011322
PC(18:0/11:1(10E))	699.3982849	1.484629256	LMGP01010735
PC(12:0/18:4(6Z,9Z,12Z,15Z))	701.6916199	0.222956068	LMGP01011326
PC(10:0/20:0)	713.9262695	1.332221436	LMGP01010395
PC(13:0/18:4(6Z,9Z,12Z,15Z))	718.4020233	2.416812887	LMGP01011351
PC(14:0/18:4(6Z,9Z,12Z,15Z))	734.6452637	50.92343205	LMGP01010499
PC(14:0/18:3(9Z,12Z,15Z))	735.803833	57.74795118	LMGP01010497
PC(14:0/18:2(11Z,14Z))	738.2484741	1.165634299	LMGP01010494
PC(14:0/18:1(11Z))	741.1770325	0.763261748	LMGP01010490
PC(13:0/20:5(5Z,8Z,11Z,14Z,17Z))	744.3664246	1.517228029	LMGP01011357
PC(15:0/18:1(11Z))	754.477356	0.833595162	LMGP01010541
PC(12:0/22:6(4Z,7Z,10Z,13Z,16Z,19Z))	757.8933716	0.830715782	LMGP01010447
PC(14:0/20:4(5Z,8Z,11Z,14Z))	762.9011078	31.29192158	LMGP01010506
PC(16:0/18:2(10E,12Z))	765.7141113	16.23479689	LMGP01010585
PC(10:0/24:0)	770.1452637	2.13800887	LMGP01010400
PC(15:0/20:3(8Z,11Z,14Z))	778.9407043	1.169170041	LMGP01011423
PC(16:0/20:4(5Z,8Z,11Z,14Z))	789.7157288	37.82410851	LMGP01010007
PC(15:1(9Z)/22:4(7Z,10Z,13Z,16Z))	801.9890137	1.363450938	LMGP01011460
PC(17:0/20:4(5Z,8Z,11Z,14Z))	804.8378601	0.448589654	LMGP01010003
PC(16:0/22:6(4E,7E,10E,13E,16E,19E))	814.1509705	1.124265111	LMGP01010650
PC(16:0/22:4(7Z,10Z,13Z,16Z))	818.4989014	1.446115056	LMGP01010642
PC(18:0/20:3(5Z,11Z,14Z))	821.5475159	1.178012109	LMGP01010795
PC(17:1(9Z)/22:6(4Z,7Z,10Z,13Z,16Z,19Z))	826.6335449	43.84880809	LMGP01011550
PC(18:4(6Z,9Z,12Z,15Z)/22:6(4Z,7Z,10Z,13Z,16Z,19Z))	835.464447	1.54416391	LMGP01011730
PC(18:3(6Z,9Z,12Z)/22:6(4Z,7Z,10Z,13Z,16Z,19Z))	836.2970886	1.422869593	LMGP01011670
PC(18:2(9Z,12Z)/22:6(4Z,7Z,10Z,13Z,16Z,19Z))	838.7856903	2.5963024	LMGP01010947
PC(18:0/22:4(7Z,10Z,13Z,16Z))	847.0201721	42.56806052	LMGP01010813
PC(16:0/24:1(15Z))	852.4560547	0.756871684	LMGP01010659
PC(20:2(11Z,14Z)/22:6(4Z,7Z,10Z,13Z,16Z,19Z))	867.4215088	1.056135248	LMGP01011865
PC(20:1(11Z)/22:6(4Z,7Z,10Z,13Z,16Z,19Z))	868.4871216	1.518624943	LMGP01011834
PC(20:0/22:4(7Z,10Z,13Z,16Z))	873.7175903	1.454865821	LMGP01011804
PC(18:0/24:1(15Z))	880.6356201	1.500554735	LMGP01010826
PC(16:0/26:0)	882.6246948	0.947456718	LMGP01010663

	m/z*	Amount, pmol per Species/μg protein	LIPIDMAPS ID
PC(21:0/22:6(4Z,7Z,10Z,13Z,16Z,19Z))	884.5966187	0.994330628	LMGP01010004
PC(21:0/22:4(7Z,10Z,13Z,16Z))	889.1891479	0.273602214	LMGP01011979
PC(22:2(13Z,16Z)/22:6(4Z,7Z,10Z,13Z,16Z,19Z))	894.450531	1.460927121	LMGP01012065
PC(22:1(11Z)/22:2(13Z,16Z))	905.4901733	1.428776634	LMGP01012032
PC(22:1(13E)/22:1(13E))	906.8718414	2.833697169	LMGP01011108
PC(18:0/26:0)	910.887207	0.778367357	LMGP01010828
PC(23:1(9Z)/23:1(9Z))	927.9228668	2.87855425	LMGP01011141
PC(22:0/24:1(15Z))	936.1557312	0.531377092	LMGP01011105
PC(20:0/26:0)	938.6951904	0.372342145	LMGP01011034
PC(24:1(15Z)/24:1(15Z))	950.0507507	121.4692795	LMGP01011163
PC(22:0/26:0)	965.9285583	1.449679534	LMGP01011107
PC(34:0/16:0)	984.3062998	7.685921442	LMGP01011218
Phosphatydilserines			
Grade 1			
PS(12:0/0:0)	440.4143036	2793.388271	LMGP03050008
PS(6:0/6:0)	457.8782501	772.5812763	LMGP03010020
PS(14:0/0:0)	470.6537933	2681.892134	LMGP03050009
PS(15:1(9Z)/0:0)	480.2579575	2310.389423	LMGP03050015
PS(16:0/0:0)	496.9708455	365.5803313	LMGP03050002
PS(18:1(9Z)/0:0)	522.1900024	1940.676303	LMGP03050001
PS(19:1(9Z)/0:0)	535.2797623	850.3865587	LMGP03050019
PS(20:4(5Z,8Z,11Z,14Z)/0:0)	545.4216919	111.6436172	LMGP03050007
PS(10:0/10:0)	565.9069214	1667.852742	LMGP03010022
PS(12:0/12:0)	622.0140991	175.9625895	LMGP03010027
PS(12:0/13:0)	638.8652649	268.9540205	LMGP03010001
PS(12:0/14:1(9Z))	653.2467041	153.7468114	LMGP03010046
PS(14:0/12:0)	654.826416	285.2899071	LMGP03010931
PS(12:0/15:0)	663.7553711	79.64711642	LMGP03010047
PS(14:0/14:0)	675.4645996	45.88818134	LMGP03010028
PS(12:0/17:2(9Z,12Z))	686.1657104	131.8011401	LMGP03010052
PS(12:0/17:1(9Z))	686.7450867	376.4542771	LMGP03010051
PS(12:0/17:0)	693.3683065	150.2897921	LMGP03010050
PS(12:0/18:2(9Z,12Z))	699.5421143	140.4609379	LMGP03010053
PS(13:0/18:2(9Z,12Z))	714.3778687	25.41099612	LMGP03010078
PS(17:0/14:1(9Z))	718.2476654	122.289291	LMGP03010006
PS(12:0/19:0)	726.2710266	42.10891676	LMGP03010057
PS(16:0/16:0)	735.1644775	569.4678808	LMGP03010029
PS(12:0/21:0)	748.2671509	1740.017591	LMGP03010064
PS(16:0/18:1(11Z))	761.6001587	22.96151068	LMGP03010007
PS(13:0/22:1(11Z))	770.7945557	2.285220437	LMGP03010089
PS(13:0/22:0)	775.6061401	94.64329165	LMGP03010088
PS(18:2(9Z,12Z)/18:2(9Z,12Z))	781.9361877	112.3843186	LMGP03010023

	m/z*	Amount, pmol per Species/μg protein	LIPIDMAPS ID
PS(17:0/20:4(5Z,8Z,11Z,14Z))	795.7001953	998.0748387	LMGP03010003
PS(16:0/22:6(4Z,7Z,10Z,13Z,16Z,19Z))	804.4544678	88.11515529	LMGP03010043
PS(18:0/20:4(5Z,8Z,11Z,14Z))	806.6505737	97.02972519	LMGP03010039
PS(18:0/22:6(4Z,7Z,10Z,13Z,16Z,19Z))	836.5066528	322.1845042	LMGP03010040
PS(18:0/22:1(11Z))	845.3986003	1022.9785	LMGP03010320
PS(19:0/22:0)	865.8910522	257.3924868	LMGP03010475
PS(20:0/22:1(11Z))	870.6346842	168.337861	LMGP03010525
PS(22:6(4Z,7Z,10Z,13Z,16Z,19Z)/22:6(4Z,7Z,10Z,13Z,16Z,19Z))	883.2276306	84.36108425	LMGP01030017
PS(22:4(7Z,10Z,13Z,16Z)/22:6(4Z,7Z,10Z,13Z,16Z,19Z))	888.2210693	100.7549591	LMGP01030018
PS(22:0/22:1(11Z))	902.2740682	739.7834825	LMGP03010722
PS(22:0/22:0)	908.0455933	99.37037004	LMGP03010943
PS(8:0/8:0)	1535.316406	3393.87959	LMGP03010021
Grade 2			
PS(6:0/6:0)	456.8153992	30698.24075	LMGP03010020
PS(14:0/0:0)	465.2920074	203.8807057	LMGP03050009
PS(15:1(9Z)/0:0)	484.0389252	1108.446661	LMGP03050015
PS(16:0/0:0)	494.9042969	52469.15679	LMGP03050002
PS(17:2(9Z,12Z)/0:0)	505.7750702	25458.10288	LMGP03050016
PS(18:1(9Z)/0:0)	522.9552917	27456.93029	LMGP03050001
PS(20:4(5Z,8Z,11Z,14Z)/0:0)	544.1977437	2318.998246	LMGP03050007
PS(20:0/0:0)	553.0429688	526.7623955	LMGP03050012
PS(10:0/10:0)	569.5486145	9698.171378	LMGP03010022
PS(22:6(4Z,7Z,10Z,13Z,16Z,19Z)/0:0)	572.4798279	8951.025196	LMGP03050013
PS(22:1(11Z)/0:0)	582.1560364	16767.76244	LMGP03050023
PS(12:0/12:0)	624.1285095	4540.48997	LMGP03010027
PS(12:0/14:1(9Z))	650.6720479	19941.5584	LMGP03010046
PS(12:0/15:0)	669.9039307	514.3605395	LMGP03010047
PS(12:0/17:0)	697.3886719	5536.324964	LMGP03010050
PS(12:0/18:2(9Z,12Z))	700.0890503	472.5421882	LMGP03010053
PS(17:0/14:1(9Z))	721.6215363	26279.15042	LMGP03010006
PS(16:0/16:0)	737.6786804	4369.155673	LMGP03010029
PS(13:0/20:2(11Z,14Z))	741.8208008	1566.624098	LMGP03010084
PS(13:0/20:1(11Z))	742.5445557	985.938965	LMGP03010083
PS(12:0/21:0)	751.5957794	18965.41756	LMGP03010064
PS(16:0/18:1(11Z))	764.1244914	4240.293661	LMGP03010007
PS(13:0/22:0)	775.519104	119.9065759	LMGP03010088
PS(18:2(9Z,12Z)/18:2(9Z,12Z))	787.125	665.3150824	LMGP03010023
PS(18:0/18:1(9Z))	791.3975525	12003.57914	LMGP03010025
PS(17:0/20:4(5Z,8Z,11Z,14Z))	797.8404948	3217.740952	LMGP03010003
PS(16:0/22:1(11Z))	820.0691732	3110.351725	LMGP03010199
PS(18:0/22:6(4Z,7Z,10Z,13Z,16Z,19Z))	839.9198608	1050.759611	LMGP03010040
PS(18:0/22:1(11Z))	845.3218384	2133.385921	LMGP03010320

	m/z*	Amount, pmol per Species/μg protein	LIPIDMAPS ID
PS(19:0/21:0)	851.4665375	29861.94664	LMGP03010474
PS(19:0/22:1(11Z))	854.967041	1085.657158	LMGP03010476
PS(20:0/22:1(11Z))	870.8126221	3280.083414	LMGP03010525
PS(21:0/22:0)	889.1227112	1632.461271	LMGP03010698
PS(22:0/22:2(13Z,16Z))	896.3721924	1235.249654	LMGP03010723
PS(22:0/22:1(11Z))	901.10554	2192.570608	LMGP03010722
PS(8:0/8:0)	1023.023682	19258.31146	LMGP03010021